Mosaicking of Orthorectified Aerial Images

Yehuda Afek and Ariel Brand

Abstract

Aerial photographs are widely used in surveying, geographic information systems (GIS), and other applications. Analysis of a large area requires the creation of an image mosaic, which is composed of several aerial photographs. In an ideal situation, a perfect mosaic can be generated using a series of rigid transformations on the source images. In practice, geometric distortions and radiometric differences interfere with the mosaicking process.

In this paper a complete algorithm to mosaic images taken at different times and conditions with geometric distortions and radiometric differences is presented. The algorithm, which works without any human intervention, integrates global feature matching algorithms into the process of selecting a seam line. The algorithm may be applied to mosaic any set of images for which an appropriate matching algorithm exists.

The creation of an image mosaic is accomplished using local transformations along a computed seam line and a rigid transformation elsewhere. An automatic stereo matching algorithm, originally developed for surface height measurement, is used to detect matching pairs of tie points across frame boundaries. These tie points are used to compute the seam line for the mosaic, and to compute geometric and radiometric correcting transformations around this seam line.

Introduction

Mosaicking is the combination of several image frames into an image mosaic covering a large area. Such mosaics can be used, among other applications, for map making (Moik, 1980).

Aerial photographs are a common source for creating photo mosaics. When transformed to any local coordinate system (e.g., UTM) and then mosaicked, the result is an orthophoto map sheet. The transformation of the photograph to a local coordinate system (Moik, 1980) is also called orthorectification. Such a transformation attempts to remove the geometric distortions that exist in a conventional aerial photograph, caused, for example, by distortions in the optical system and by the perspective projection.

The transformation depends on *a priori* knowledge about the optical system, the camera position and attitude at the time of photography, and the surface elevation at each point visible in the photograph. This *a priori* knowledge is usually known with limited accuracy. In particular, the surface elevation is usually available only at grid points, with interpolation being used for points between grid points. These inaccuracies cause distortions in the final orthorectified aerial photograph. These distortions cause features in the map plane to appear at incorrect locations with respect to their true geographic location.

The geometric distortions added during the orthorectification process vary for different photographs, for example, due to the use of different cameras and due to inaccuracies in the ground elevation data used to correct the perspective projection. Therefore, the same feature appearing in two different photographs might appear in different map plane coordinates in the two orthorectified images created from both photographs. This distortion prevents the simple mosaicking of the two orthorectified images by a simple two-dimensional rigid transformation.

In addition to the geometric distortions, radiometric differences between adjacent photographs must also be handled to create a seamless mosaic. These differences are caused by sun-angle-dependent shadows; seasonal changes of fields, forests, and water bodies; different atmospheric conditions; and variations during film development.

In mosaicking two images, most systems define a seam line. The seam line goes across the overlap area between tie points, which are points that correspond to the same set of features in the two overlapping images. Along this line the images are tailored together by locally matching them geometrically and radiometrically. Common photogrammetric software for performing image mosaicking requires that a human operator identify pairs of tie points along the operator selected seam line, that is, pairs of points in the two images that represent the same feature.

The main contribution of this paper is in the integration of global feature-matching algorithms into the process of automatic seam-line selection. In existing digital photogrammetric systems, the process of identifying matching tie points and selecting the seam line is done manually, sometimes with the aid of a local matching algorithm. In this paper (see Figure 1), the system first performs a global matching algorithm to automatically identify many potential pairs of tie points in the overlap area, and then proceeds to select a seam line using a subset of these points. This process has several advantages over manual or semi-automated systems:

- The seam line is selected here from a large set of matched potential tie points. This enables us to use sophisticated techniques to select the line along pairs of points while taking into consideration the amount of geometric and radiometric distortion. The seam line thus selected is both locally appropriate for tailoring the two images and minimizes the accumulated distortion along the line.
- Because we use a global matching algorithm to find all the potential tie points in one shot, the computational overhead of the process is minimized, compared to the overhead introduced by local matching used in semi-automated systems. This is because in semi-automated systems the local matching starts from scratch several times on neighboring territories.

Several tools from stereo photogrammetry/pattern matching and graph theory are used in the above process. For the global matching algorithm we have adapted the algorithm of Brookshire *et al.* (1990). The algorithm for selecting the seam

Computer Science Department, Tel-Aviv University, Israel 69978.

Photogrammetric Engineering & Remote Sensing, Vol. 64, No. 2, February 1998, pp. 115–125.

0099-1112/98/6402-115$3.00/0

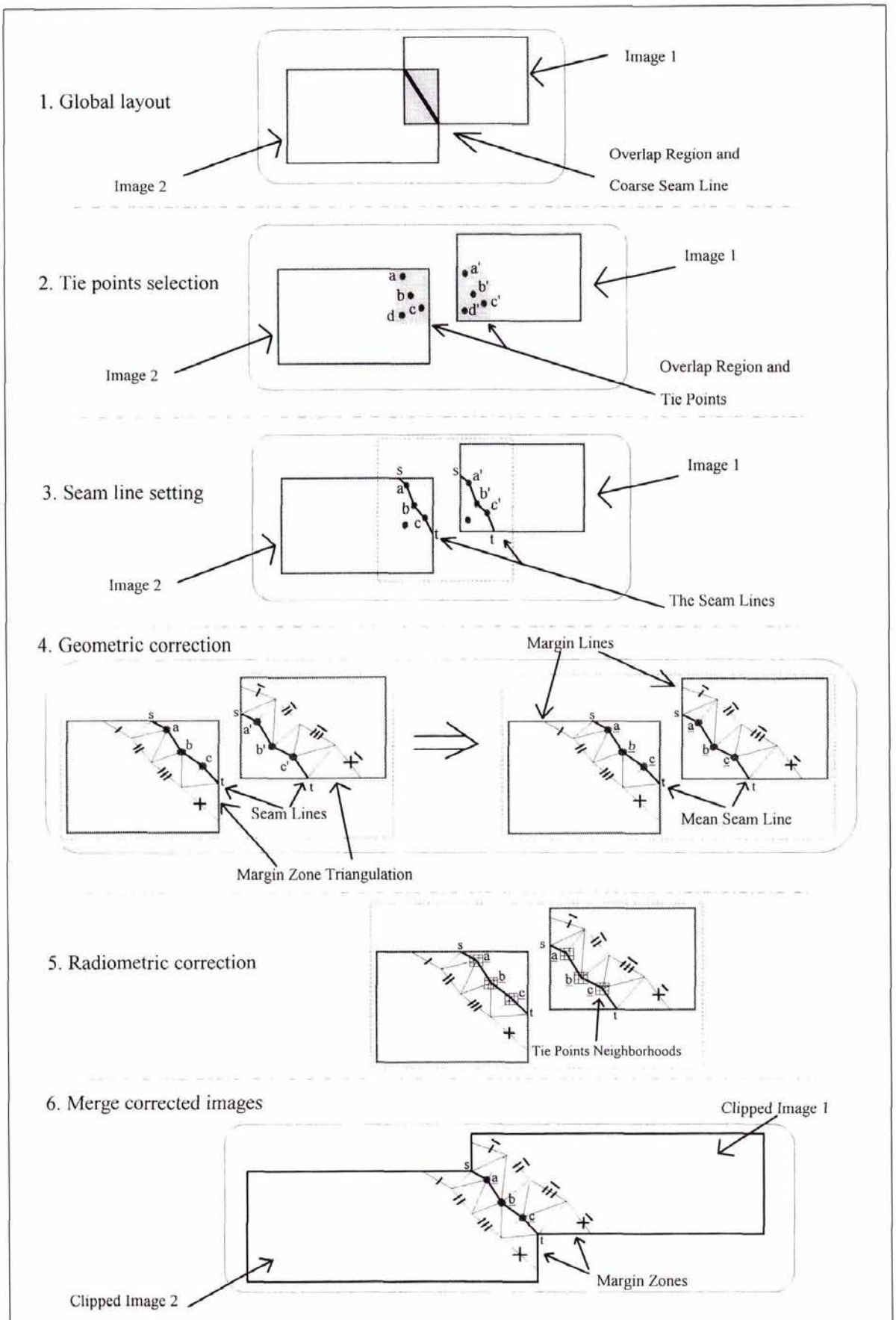

Figure 1. Algorithm overview.

line in the network of potential tie points is an iterative extension of Dijkstra's shortest path algorithm (Even, 1979).

This paper completely automates the creation of the image mosaic, including the definition of a seam line based on tie points extracted using a matching algorithm, and the performance of geometric and radiometric corrections, yielding a seamless mosaic.

Related Work

The subject of creating an image mosaic was originally managed using photomechanical devices (Mullen, 1980). Creating a mosaic in this manner is labor intensive and can't handle local distortions in the different images. Non-digital mosaicking is still in use (Vickers, 1993). The trend toward digital photogrammetry (Boniface, 1992) required the development of digital mosaicking algorithms. Such algorithms were developed both for photographic images (Zobrist *et al.*, 1983) and for synthetic aperture radar images (Wivell *et al.*, 1993; Schultz *et al.*, 1989).

The photographic image mosaicking algorithms address two different problems: smoothing geometric and radiometric discontinuities in adjacent images, and choosing the best image source at each point. The latter problem is caused, e.g., by different cloud coverage in each of the images (Nakayama and Tanaka, 1990).

In this paper, we address the problem of smoothing geometric and radiometric discontinuities in adjacent images. One type of mosaicking algorithm assumes that no geometric or radiometric corrections are needed. These algorithms merely select a seam line that yields the best results for the rigid transformation mosaicking procedure (Hummer-Miller, 1989; Shiren *et al.*, 1989). Zobrist *et al.* (1983) performed geometric and radiometric corrections along seam lines selected by the operator. Automatic correlation enhanced the detection of tie points along the seam line. This algorithm was used for orthophoto production (Hood *et al.*, 1989). Another algorithm (Albertz *et al.*, 1992) added contrast correction to the traditional intensity correction.

In this paper, tie points are first extracted in the images' overlap region, and then the seam line is selected by an automatic procedure. This avoids the need for manually selecting the seam line, and enables the use of automatic matching algorithms that are not restricted to work on pre-defined search windows. Such matching algorithms were developed for use in various applications (Perlant and McKeown, 1990). This enhancement yields a seam line that contains many known tie points and, thus, improves the final quality of the resulting mosaic.

The Model

Aerial photographs give a two-dimensional representation of the three-dimensional world. This representation is based on a perspective projection. In a perspective projection the image scale, that is, the ratio between size in the two-dimensional image and the three-dimensional world, is not constant. This prevents the correct measurement of real distances and angles using the aerial photograph.

Cartographic maps give a two-dimensional representation of the three-dimensional world that have a constant scale. It is thus possible to measure distances and angles on the cartographic map. Orthorectification is the process that transforms an aerial photograph from a perspective projection to a cartographic map projection. The result of this process is an orthorectified image.

Every digital orthorectified image is a geocoded raster image file. The geocoding information is a transformation from the image pixels to the cartographic map-plane coordinates. In this paper, only gray-level images are used. Real image data versus empty regions of the image file are explicitly expressed using a bounding polygon, with vertices given in the map-plane coordinates. The geocoding transformation includes translation and scaling. Resampling must be used for images of different scales.

Algorithm Overview

The mosaic algorithm is based on six major stages, as depicted in Figure 1:

(1) *Global Layout.* The first stage handles the global elements. It identifies the overlapping region of the two input images. An intersection of the images bounding polygons yields this overlap, and the geocoding information (assignment of map-plane coordinates to pixels) enables the transformation of polygonal lines to the image pixels. In addition, the first stage also sketches a rough line in whose neighborhood the final seam line will be located, and, for each image, the image side of the seam line to be kept in the mosaic is identified.

(2) *Tie Point Selection.* The second stage extracts the tie points. This is done using a matching algorithm. For this paper, a stereo matching algorithm, originally designed for the measurement of surface height based on image parallax, is used (Brookshire *et al.*, 1990). That algorithm was originally designed to manage aerial photographs. The selection of tie points need not create a regular grid, nor be of some specific density.

(3) *Seam Line Setting.* The third stage performs the exact selection of the seam line. This line is actually a pair of polylines, each representing a polyline in one of the input images. These polylines should run along corresponding objects and features in the two images. The selection is done using iterations of a Dijkstra algorithm for finding the shortest path between the images' tie points in a weighted graph. The weights of edges connecting tie points factor in several parameters that effect the quality of the mosaic. These parameters include the distance between tie points, the distance to the coarse seam line, and the relative deformation between successive pairs of points.

(4) *Geometric Correction.* The fourth stage performs the geometric correction. The final coordinates of each seam line point are computed as the average of its two counterpart tie points coordinates. This results in three seam lines, one in each image and the one along which the two images are pasted together. In the correction process some area along the seam line is stretched (or shrunk) to bring its seam line to the pasting line.

To perform this correction, a margin line is first built in each image parallel to the seam line and at a predetermined distance from the seam line. As the spatial quality of the image deteriorates, a larger distance is necessary (in our implementation, this distance was set at 100 pixels). The area enclosed between the seam line and the margin line is the margin zone. This zone is next partitioned into triangular regions. Each triangle is given two sets of vertices, one set representing the triangle vertices before the correction, and the other after. A raster copy operation, based on the Feibush Levoy Cook algorithm (Foley *et al.*, 1990), is then used to copy the imagery from the area covered by the triangle with the first set of vertices to the one with the second set of vertices. This is done by computing the pixels intensities in the output triangle using bilinear interpolation of the pixels intensities in the input triangle. If the polylines of the seam line are reselected along the same features in the images after the geometric correction, the two new polylines will have the exact same map-plane coordinates for all corresponding pairs of points. This ensures the perfect matching of the two images when mosaicked along the pasting line.

(5) *Radiometric Correction.* The fifth stage handles the radiometric corrections necessary to create a seamless mosaic. The correction is again based on triangulating an interest area along the seam line as in the previous stage. For each triangle, radiometric correction parameters are computed

based on image gray values at tie point neighborhoods. These parameters aim to bring both the images' average gray level and standard deviation to equal values on both sides of the seam line. The result gives both images a common radiometric appearance along the seam line.

(6) *Merge Corrected Images.* To complete the mosaic, all that is necessary is to build a new image file, i.e., the merged image of the two unchanged regions of the input images and the two modified margin zones. This can now be accomplished using four copy operations, taking into consideration the geocoding information. Data from only one image will be taken for each side of the seam line, and the geometric correction stage ensures that there is no overlap along the seam line.

Global Layout

Each input image contains the actual raster data, the geocoding information, and a bounding polygon (given in map-plane coordinates). This last polygon specifies the separation of the image pixels between those that have a null value, or otherwise contain irrelevant data, and those that actually contain photographic data.

To enable the mosaicking of two input images, the mutual location of the two images on the map projection plane must be determined. This information is easily extracted from the two bounding polygons. The images' mosaic will cover the area bounded by the union of the two images bounding polygons. The actual union can be computed by the Weiler polygon clipping algorithm (Foley *et al.*, 1990).

Apart from the general region in which the mosaic will take place, a general path for the seam line must also be computed. Later on, this coarse selection will be refined in the final selection of the seam line. Usually, the task of selecting a coarse path for the seam line is better done by a human operator. This is due to the need to inspect the images in many aspects, such as cloud coverage, blur versus sharp image sections, dense areas versus open spaces, and so on. All these are hard to account for in an automatic procedure, and were not handled in this paper.

The actual selection of a coarse path for the seam line is done by selecting a line stretching between the intersection points of the input images bounding polygons. Such a line can be computed by defining a graph representing the global layout of the images and applying the Dijkstra algorithm (Even, 1979). The graph vertices include the intersection points of the images' bounding polygons, as well as all vertices of the bounding polygons. The edges of this graph will include all line segments between any two vertices that are entirely within the images' overlap region.

The overlap region can again be computed using the Weiler polygon clipping algorithm. The weight of each edge is the Euclidean length of the line segment between the vertices connected by the edge. The graph and the selected coarse seam line are demonstrated in Figure 2 for two examples. The selection of a path using the Dijkstra algorithm ensures the selection of the shortest possible coarse seam line.

Tie Point Selection

The tie point selection algorithm used in this paper is based on an article by Brookshire *et al.* (1990). The algorithm was developed to solve the stereophotogrammetry problem by measuring the image parallax of two stereo images and using this measure to compute the ground elevation. However, the algorithm is more general and solves the problem of matching two images with relative distortions in arbitrary directions. Other matching algorithms, such as that by Medioni and Nevatia (1985) or by Weng *et al.* (1992), may also be used with no modifications required at other stages of the mosaicking algorithm.

The algorithm refines the disparity map by matching corresponding topological features at successively finer resolutions as shown in Figure 3. First, the original images are reduced to the desired pseudo-hex resolution. Then an edge-vector operator (Bowker, 1974) is applied to produce a full edge-vector field. Next, the threshold and association operators thin the vector field to its most prominent edges. The node operator is then applied to both associated edge-vector fields. For each node in image 1, the matching algorithm searches a small hexagonal window in image 2 for candidate matching nodes and correlates the local edge-vector fields to find a match. The disparity network from the matches is then filled in by a spatial interpolation, expanded to the next resolution size, and then filled again by interpolation. These steps are repeated at pseudo-hex resolutions 54, 18, 6, and 2. At the original gray-scale level a modified, normalized cross-correlation (Duda and Hart, 1973) on small windows provides the final disparity network. In principal, the matching points found can be further refined to sub-pixel precision using an algorithm such as that by Lyvers *et al.* (1989).

Seam Line Setting

The tie points identified during the matching stage are scattered all over the images. The next task is to build a seam line for the mosaic based on these tie points. The seam line end points were found during the global layout stage, but the specific path must yet be selected.

Selecting a seam line is actually the selection of a set of tie points. The polyline running between these points will serve as a seam line. Geographically the lines selected for both images are equal, but in the map projection plane they differ due to the geometric distortions. Our aim is to select such a set of tie points that will enable good application of the geometric correction.

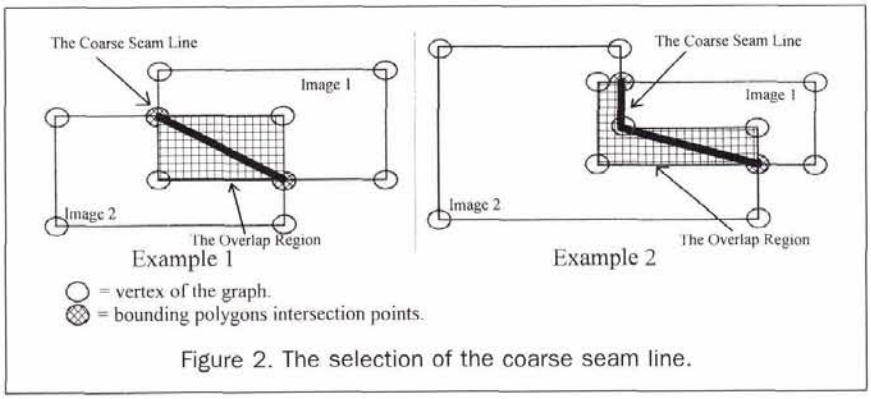

Figure 2. The selection of the coarse seam line.

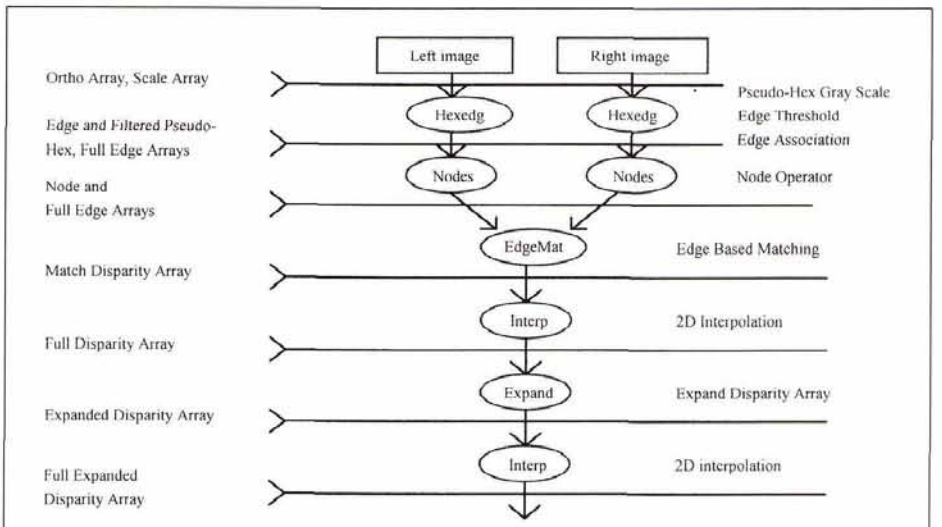

Figure 3. Matching algorithm applied at each resolution.

To support the selection of the seam line, we first need to define the considerations for selecting a seam line that will best serve the geometric correction stage. Four such considerations are currently handled, and a fifth one may be considered. The four include

- Having short distances between adjacent points,
- Minimizing the distance of the points from the coarse seam line,
- Selecting tie points at areas of small geometric distortion, and
- Selecting tie points with minimal variations of geometric distortion between adjacent pairs.

The fifth consideration that may be added is the selection of well-identified tie points, assuming that the matching algorithm has the capability of giving each tie point a figure of merit, indicating the match reliability.

Short distances between adjacent points are required because our best estimate of the geometric distortion along the seam line is just a linear interpolation of the distortions at the selected tie points. Selecting widely separated points gives a very poor estimate of the real distortion. Correcting the image based on such an estimate yields a poor mosaic.

Selecting points near the coarse seam line is essential for taking into account the considerations used in selecting the coarse line. These include, e.g., using a short seam line or crossing areas with less distinct features, where the geometric correction is less likely to be observable.

The third consideration aims to minimize the magnitude of the required geometric correction. The fourth consideration attempts to ensure that the geometric correction at adjacent points has approximately the same direction and magnitude. This minimizes the geometric shifts added to the image by the mosaicking process and improves the mosaic quality.

Now that we have stated the considerations that need to be taken into account in the selection of the seam line, we need a method for actually selecting the tie points of the seam line. To perform this, a modified Dijkstra algorithm is used. The standard Dijkstra algorithm (Even, 1979) answers the single source shortest path problem in directed graphs, where each edge of the graph has a positive constant weight. A modified algorithm will be used because the edges' weights in our problem are not constant.

The graph $G = (V, E)$ to be used will be built in the following manner:

- Each tie point will serve as a vertex.
- An edge between any two tie points will be defined that is not too far apart, nor too close. For any such pair of points, two edges will be added to E, one in each direction.
- The weight for a given edge will be a weighted sum of the four previously described considerations.

Selecting points too close together in any of the images will cause a distortion during the geometric correction. Points too far apart are not used mainly for practical reasons, i.e., to avoid n^2 number of edges. Because of this, problems might arise if the seam line crosses areas that could not be correlated, such as lakes, in which no tie points are identified. Currently, semi tie points are used to solve this problem, but a dynamic method may also be used, demanding, for example, that any vertex will have at least one outgoing edge in any 30° pie slice around it, regardless of how long this edge might be.

The weight $w(e)$ for a given edge $e \in E$, connecting the points $u = (ux, uy)$ and $v = (vx, vy)$ in the first image, and points $u' = (ux', uy')$ and $v' = (vx', vy')$ in the second image (Figure 4), will be a weighted sum of the quantities $w_i(e)$, each representing one of the previously described considerations: i.e.,

(1) $w_1(e) = \|u - v\|^4$,

(2) $w_2(e)$ = the distance of u to the coarse seam line,

(3) $w_3(e) = \|u' - u\|$, and

(4) $w_4(e) =$

$$\sqrt{[(vx' - vx) - (ux' - ux)]^2 + [(vy' - vy) - (uy' - uy)]^2}.$$

Having four different quantities to contribute weight for a single edge forces us to set the final edge weight as a weighted sum of these quantities. To select the coefficients of the weighted sum, we use an iterative process. This process adjusts the coefficients after each computation of a seam line (using a regular Dijkstra algorithm). The adjustments are repeated several times. The adjustments may stop once the total contribution of each of the four computations to the line selection is about equal. This process is outlined in Algorithm 1 (Appendix A).

The described algorithm may easily be modified to have each quantity contribute a different amount to the final seam

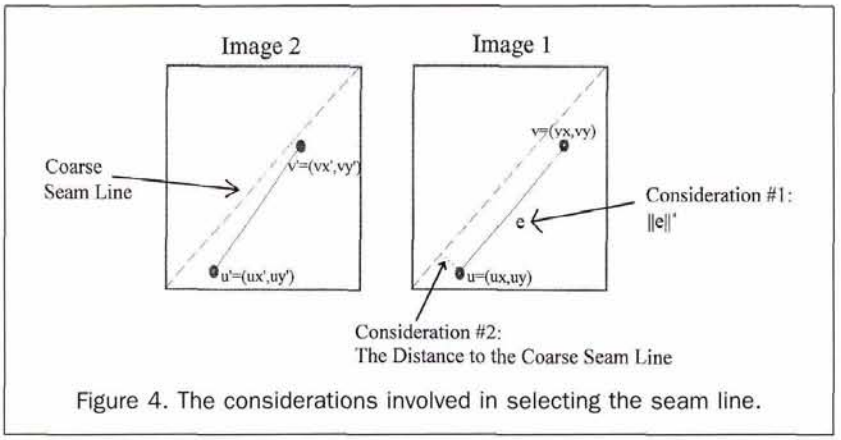

Figure 4. The considerations involved in selecting the seam line.

selection, or even to handle more quantities, such as the matching algorithm figure of merit.

For optimal operation, the Dijkstra algorithm is implemented using a Fibonnaci Heap (Kozen, 1992).

Geometric Correction

The geometric correction stage is built of three major steps:

- Defining a margin zone for the correction;
- Triangulating the margin zone; and
- Transforming the image, using the triangulation, to the corrected form.

Defining a Margin Zone

The margin zone marks the region in which corrections may be made. This zone will generally be a limited strip along the seam line (see Figure 5). The width of the margin zone should be proportional to the magnitude of the distortions in the images. This ensures moderate image shifts during the geometric correction, and also avoids changing the images at unnecessary positions.

The formation of the margin zone is not a simple task. The seam line itself is built of many short line segments pointing in random directions. To define the margin zone, a line parallel to the seam line, at some distance d from the seam line, is required. The simple method of drawing a line segment parallel to each line segment of the seam line yields poor results, as seen in Figure 6. Better ways can be used, both in the raster and in the vector domains.

In the raster domain, defining the margin line can be accomplished using algorithms that compute the distance of each object pixel from the object's background (Shih and Mitchell, 1992). It is thus possible to collect all pixels at distance d from the object's background. In this case, the seam line itself is the background, the rest of the image being the object.

In the vector domain, this can be done by defining a bounding rectangle around each segment of the seam line and using the union of all these rectangles. The outer polygon line thus created, not including the seam line itself, is the margin line (see Figure 7).

Triangulating the Margin Zone

The triangulation of the margin zone is done by finding the nearest point on the margin line for each seam line point, and splitting the area surrounded by two adjacent seam line points and their counterparts on the margin line into two triangles. Special care is taken at the two sides of the margin zone, to prevent defining a triangle over an area that is not within the margin zone. This process yields a series of triangles, with no overlaps, that cover the entire margin zone (see Figure 8a).

Correcting the Margin Zone

The final, and most important, step in the geometric correction is the actual application of a transformation to the image pixels. To do this, we define a new set of triangles that match the triangles just created. These triangles are defined by first copying the original set of triangles, and then changing the position of each vertex of a triangle that is on the seam line to the position of this point after the correction. This position is basically computed as an average of the pair of points constituting the tie point at this position of the seam line (see Figure 8b).

For each pair of triangles, it is now possible to copy the image data from the source image to the corrected target image using the Feibush Levoy Cook raster copy algorithm. In this algorithm, a target-to-source transformation is computed, based on interpolations of the known end points of the re-

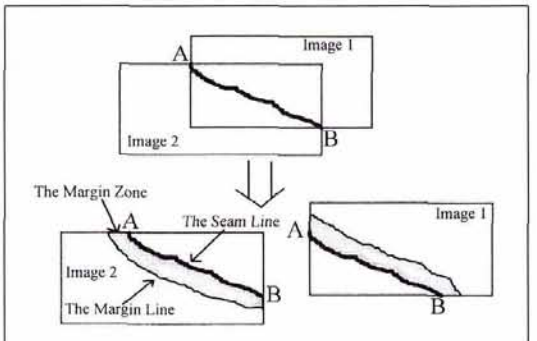

Figure 5. The margin zone.

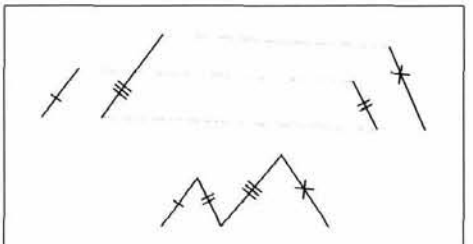

Figure 6. Naive margin zone formation.

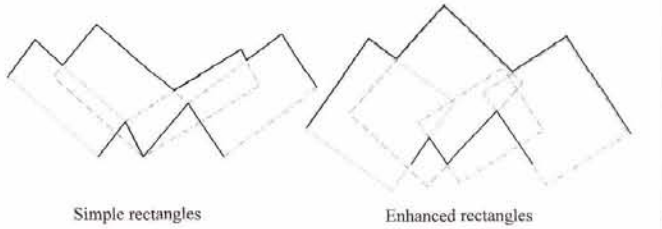

Figure 7. Improved margin zone formation.

gion (in this case, a triangle), as depicted in Figure 9. Next, for each pixel in the target image that falls within the bounds of the triangle, the transformation is used to find the position in the source image from which this pixel should be taken. The actual sampling of the data is done using a bilinear interpolation.

Radiometric Correction

The two images being mosaicked may have different pixel gray values along the selected seam line, even if global image enhancement was used prior to the mosaicking. Our goal in doing a radiometric correction is to diminish the radiometric differences along the seam line.

Two radiometric features will be modified. These include image intensity and contrast. Intensity is taken as the gray-level average in a point neighborhood. Contrast is taken as the value of the standard deviation of the gray levels in such a neighborhood.

Due to the availability of the tie points, it is possible to compute both the radiometric intensity and contrast (average and standard deviation) for corresponding pairs of points in the two input images. Figure 10 shows the neighborhoods of corresponding tie points on the seam line. Having the corresponding average and standard deviation enables one to compute the parameters for the radiometric correction. The object here is to shift both images' intensities to their intensities mathematical average, and the images' contrast to their contrast geometrical average.

The actual application of the radiometric correction is done in a manner similar to the geometric corrections, using triangles coverage of the margin zone. This zone, and the triangles used to cover it, may differ from those used in the geometric correction if needed. This may be the case if we want to narrow down the margin zone width, or if we want to use smaller triangles to improve the result.

The computation of the radiometric correction parameters for each tie point is done as shown in Algorithm 2 (Appendix B). For all other vertices, only the average gray level A is computed, and the correcting parameters are $P_1 = 1$, $P_2 = A$, and $P_3 = 0$. For all other points covered within the triangle, a linear interpolation is used between the triangle's vertices to compute the required radiometric correction parameters.

Due to the structure of the triangles, pixels that are adjacent to one another but belong to different triangles will be subject to similar radiometric corrections. This ensures the continuity of the radiometric correction.

We now need to apply the radiometric correction, based on the computed correction parameters. For each pixel covered within a triangle, there is an exact definition of the three correction parameters. The correcting computation is, then, $n = (o - P_2) \cdot P_1 + P_2 + P_3$, where n and o are the new and old pixel gray values, respectively.

Wrapping Up

The initial input for the mosaic process was two geocoded raster image files. The final output is a single geocoded image file. During the geometric and radiometric correction stages, a margin zone along the two images' seam line was modified. Now we need to build up the final image from four separate image sections. These include the two modified margin zones, as well as the remaining image data of each of the original images. To start with, we create an empty geocoded image file, large enough to hold the four required image sections. The image size can easily be determined based on a bounding rectangle of the original images' bounding polygons. The Feibush-Levoy-Cook raster copy algorithm can next be used to copy the image data. The margin zone serves as the bounding polygon to copy the modified image section. The polygon created from the image bounding polygon and the margin line is used to copy the rest of the image.

To enable further mosaicking of another image to the currently mosaicked images, we need to have the same information about the images' mosaic as for the original images. This means the newly created geocoded image file and a bounding polygon. This bounding polygon is simply the union of the original images' bounding polygons, computed using the Weiler polygon clipping algorithm.

Experimental Results

The algorithm presented in this paper was implemented and tested with real data. The test images included two sets of orthorectified aerial images, as well as a group of orthorectified satellite imagery. All images were approximately 5000

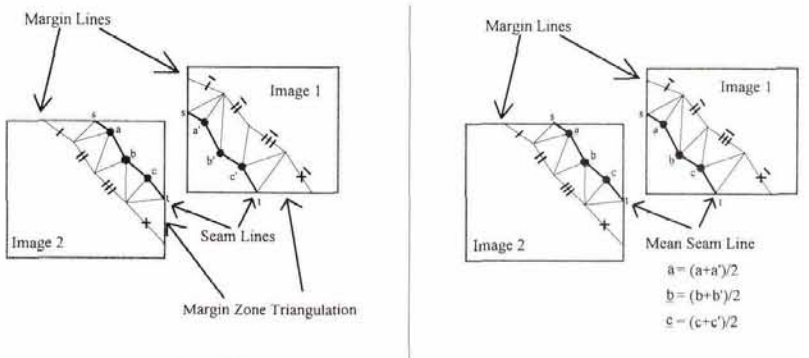

a: pre-correction triangles

b: post-correction triangles

Figure 8. Margin zone triangulation.

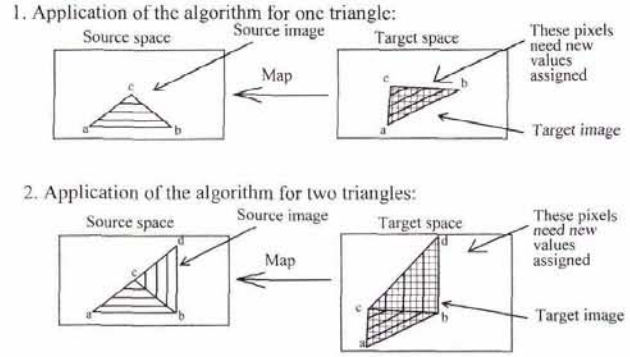

Figure 9. The relationship of the source space, source image, target space, and target image in the Feibush-Levoy-Cook algorithm.

by 5000 pixels in size. In total, more than 30 images were mosaicked. The resulting mosaicked images were reviewed both in softcopy and in hardcopy. The subjective opinion of several geodetic and photogrammetric engineers was that the results were better than those achieved with other, non-automatic, available systems.

Incorrect geometric correction was observed once, due to errors in the matching stage. Usually, even when incorrect tie points were identified, the selection of the seam line tended to ignore these incorrect tie points. The number of identified tie points was usually large enough.

It was observed that the triangulation of the margin zone for the radiometric correction gives better results when triangles of smaller width are used. The radiometric differences between adjacent pixels might differ significantly, and, therefore, the radiometric correction parameters need to be computed for a larger number of points than that used for the geometric correction.

A high resolution image is used, in Figure 11, to demonstrate the mosaicking effect. The original image was duplicated, and then slightly shifted. The mosaic algorithm pastes correctly the original and the modified images.

Figures 12 and 13 provide a reference of a simple rigid transformation mosaic algorithm, to compare with the mosaic using the algorithm suggested in this paper. The images used are image pieces extracted from 1-metre-resolution orthorectified aerial photographs. The effect of both the geometric and the radiometric corrections is visible. The circles draw attention to areas of large geometric distortion.

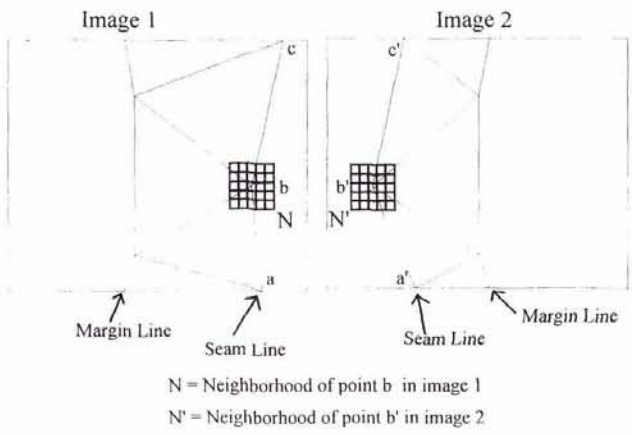

Figure 10. The neighborhoods of tie points.

Result of a simple cut & paste mosaic

Result of the suggested mosaic algorithm

Figure 11. Example 1 — Correcting an artificially introduced distortion.

Limitations

The mosaic algorithm suggested in this paper has several limitations. Some of these limitations are due to the automation of the seam line selection, while others are common to non-automatic mosaic algorithms, and may be improved using ideas existing in such algorithms.

The automatic selection of tie points and of the seam line requires a much broader overlap region than is necessary for a human operator. This is due to the limitations of today's matching algorithms. These algorithms are also not perfect, and manual verification procedures ought to be considered for the tie points used along the seam line. Another problem due to the automation of the algorithm is the simplicity of choosing the coarse path for the seam line. The automatic selection disregards many important aspects, usually considered by a human operator. This selection might also fail to understand the respective location of the mosaicked images when these intersect in a non-regular way.

Summary

In this paper an automatic algorithm for performing image mosaic of orthorectified aerial photographs that compensates

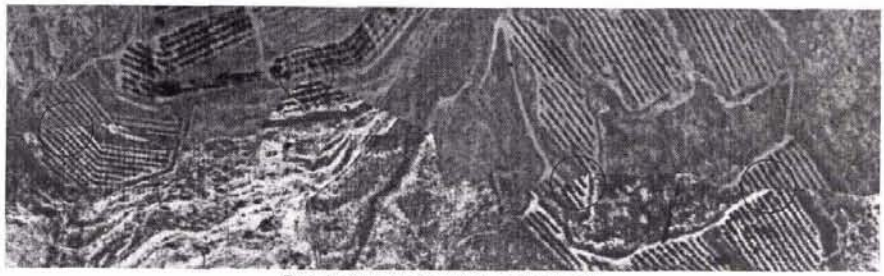

Result of a simple cut & paste mosaic

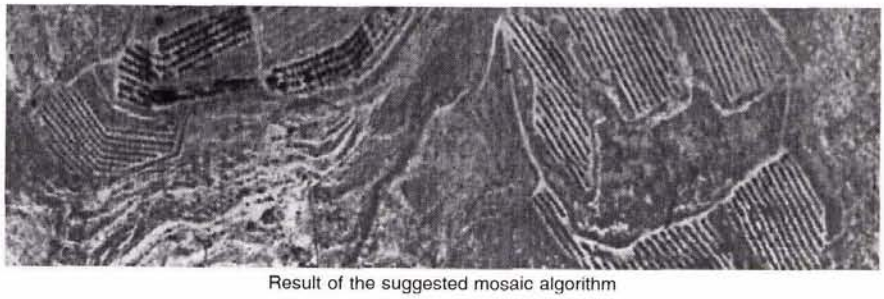

Result of the suggested mosaic algorithm

Figure 12. Example 2 — Mosaic of true orthorectified aerial photographs.

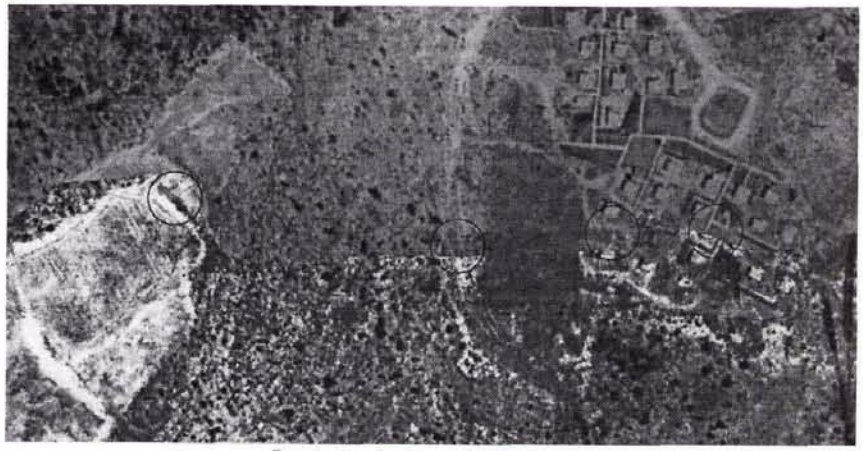

Result of a simple cut & paste mosaic

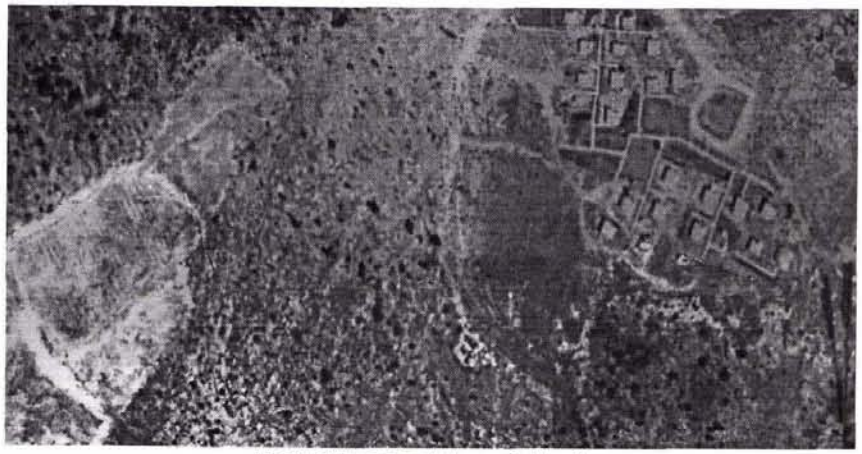

Result of the suggested mosaic algorithm

Figure 13. Example 3 — Mosaic of true orthorectified aerial photographs.

for geometric distortions and radiometric differences is presented.

The special advantage of this algorithm compared with available algorithms for doing image mosaicking is in using an automatic matching algorithm for extracting tie points. The automatic extraction greatly enhances the speed of the tie points selection stage and, hence, the overall process speed. Furthermore, it allows for a better selection of a seam line for the mosaic. Based on the experimental results, the automatically selected seam line contains many more tie points than the number of tie points a human operator would normally select. The selected seam line path is also not the path likely to be chosen by a human operator. However, the experiments support the claim that this seam line does enable the good application of the geometric correction. For example, wherever possible the line segments of one image were perfectly matched with their counterparts in the second image.

The triangulation method proved excellent both for the geometric and the radiometric correcting transformations. Accounting for both image intensity and contrast in the radiometric correction yielded a seamless mosaic even when very large radiometric differences existed in the two mosaicked images.

The complete algorithm gives an automatic capability to produce a qualitative image mosaic from multiple orthorectified aerial photographs.

References

Albertz, Jeorg, Hartmut Lehmann, Frank Scholten, and Ruediger Tauch, 1992. Satellite Image Maps — Experiences, Problems and Chances, *International Archives of Photogrammetry and Remote Sensing*, 17th Congress, 29-4:309–314.

Boniface, P.R.J., 1992. PRI2SM - Softcopy Production of Orthophotos and DEM, *Photogrammetric Engineering & Remote Sensing*, 58: 91–94.

Bowker, Kent J., 1974. Edge Vector Image Analysis, *Proceedings, Second International Joint Conference on Pattern Recognition*, IEEE, Copenhagen, pp. 520–524.

Brookshire, Greg, Morton Nadler, and Choon Lee, 1990. NOTE: Automated Sterophotogrammetry, *Computer Vision Graphics and Image Processing*, 52:276–296.

Duda, Richard O., and Peter E. Hart, 1973. *Pattern Classification and Scene Analysis*, Wiley, New York, pp.276–284.

Even, Shimon, 1979. *Graph Algorithms*, Pitman, London, pp. 13–15.

Foley, James D., Andries van Dam, Steven K. Feiner, John F. Hughes, 1990. *Computer Graphics: Principles and Practice, Second Edition*, Addison-Wesley Publishing Company.

Hood, Joy, Lyman Ladner, and Richard Champion, 1989. Image Processing Techniques for Orthophotoquad Production, *Photogrammetric Engineering & Remote Sensing*, 55:1323–1329.

Hummer-Miller, Susanne, 1989. A Digital Mosaicking Algorithm Allowing for an Irregular join 'Line,' *Photogrammetric Engineering & Remote Sensing*, 55:43–47.

Kozen, Dexter C., 1992. *The Design and Analysis of Algorithms*, Springer-Verlag, pp. 44–47.

Lyvers, Edward P., Owen Robert Mitchell, Mark L. Akey, and Anthony P. Reeves, 1989. Subpixel Measurements Using a Moment-Based Edge Operator, *IEEE Transactions on Pattern Analysis & Machine Intelligence*, 11:1293–1309.

Medioni, Gerard, and Ramakant Nevatia, 1985. Segment Based Stereo Matching, *Computer Vision Graphics and Image Processing*, 31:2–18.

Moik, Johaness G., 1980. *Digital Processing of Remotely Sensed Images*, NASA.

Mullen, Roy R., 1980. Aerial Mosaics and Orthophotomaps, *Manual of Photogrammetry, Fourth Edition* (C. C Slama, editor), American Society of Photogrammetry, Falls Church, Virginia, pp. 761–783.

Nakayama, Y., and S. Tanaka, 1990. An Image Connection of NOAA AVHRR Data in Plural Orbits, *Proceedings, International Geoscience & Remote Sensing Symposium*, 1:651–654.

Perlant, Frederic P., and David M. McKeown, 1990. Scene Registration in Aerial Image Analysis, *Photogrammetric Engineering & Remote Sensing*, 56(4):481–493.

Schultz, Fern, J. Bryan Mercer, and Peter Button, 1989. Digital Mosaicking Technology for Synthetic Aperture Radar Image Products, *Proceedings, International Geoscience & Remote Sensing Symposium*, 1:120–123.

Shih, Frank Yeong-Chyang, and Owen Robert Mitchell, 1992. A Mathematical Morphology Approach to Euclidean Distance Transformation, *IEEE Transactions on Image Processing*, 1(2): 197–204.

Shiren, Yang, Li Li, and Gao Peng, 1989. Two-Dimensional Seam-Point Searching in Digital Image Mosaicking, *Photogrammetric Engineering & Remote Sensing*, 55:49–53.

Tian, Q., and M.N. Huhns, 1986. Algorithms for Subpixel Registration, *Computer Vision Graphics and Image Processing*, 35:220–233.

Vickers, E. Wayne, 1993. Production Procedures for an Oversize Satellite Image Map, *Photogrammetric Engineering & Remote Sensing*, 59:247–254.

Weng, Juyang, Narendra Ahuja, and Thomas S. Huang, 1992. Matching Two Perspective Views, *IEEE Transactions on Pattern Analysis & Machine Intelligence*, 14:806.

Wivell, Charles E., Coert Olmsted, Daniel R. Steinwand, and Christopher Taylor, 1993. Remote Sensing Brief: An Earth Remote Sensing Satellite-1 (ERS-1) Synthetic Aperture Radar Mosaic of the Tanana River Basin in Alaska, *Photogrammetric Engineering & Remote Sensing*, 59:527–528.

Zheng, Qinfen, 1993. A Computational Vision Approach to Image Registration, *IEEE Transactions on Image Processing*, 2(3):311–325.

Zobrist, A.L., N.A. Bryant, and R.G. Mclead, 1983. Technology for Large Digital Mosaics of Landsat Data, *Photogrammetric Engineering & Remote Sensing*, 49:1325–1335.

(Received 8 July 1996; accepted 10 March 1997; revised 10 April 1997)

Appendix A

Algorithm 1. The Iterated Dijkstra Algorithm.

$\forall_i = 1..4$, $\text{coef}_i = 1$
select source s and target t vertices nearest to the coarse seam line end points.
for loop = 1 to MAX_LOOPS do {
  $\forall_e \in E$, $w(e) = \sum_{i=1..4} w_i(e) \cdot \text{coef}_i$
  Apply Dijkstra algorithm, to compute the shortest path P, from s to t in $G = (V, E)$.
  $\forall_i = 1..4$, $\text{sum}_i = \sum_{e \in P} w_i(e) \cdot \text{coef}_i$
  $\text{total} = \sum_{i=1..4} \text{sum}_i$
  $\forall_i = 1..4$, $\text{coef}_i = \text{coef}_i \cdot \text{total}/\text{sum}_i$
  if ($\forall_i \in 1..4$, $0.2 \cdot \text{total} < \text{sum}_i < 0.3 \cdot \text{total}$) then
    break
}

Appendix B

Algorithm 2. Computing Radiometric Correction Parameters for Tie Points.

Let $I[i]$ represent the pixels array of image 1, and $I'[i]$ the pixels array of image 2.
Let N and N' be the neighborhoods of a tie point pair, $|N| = |N'|$.
Then the computation of the correction parameters for this tie point is:

$$A = \frac{1}{|N|} \sum_{i \in N} I[i];$$

$$A' = \frac{1}{|N'|} \sum_{i \in N} I'[i]$$

$$\sigma = \frac{1}{|N|} \sqrt{\sum_{i \in N} (I[i] - A)^2};$$

$$\sigma' = \frac{1}{|N'|} \sqrt{\sum_{i \in N'} (I'[i] - A')^2}$$

$$\overline{\sigma} = \sqrt{\sigma \cdot \sigma'}$$

$$\forall i \in N, \bar{I}[i] = \frac{\overline{\sigma}}{\sigma} (I[i] - A) + A;$$

$$\forall i \in N', \bar{I}'[i] = \frac{\overline{\sigma}}{\sigma'} (I'[i] - A') + A'$$

$$\overline{A} = \frac{1}{|N|} \sum_{i \in N} \bar{I}[i];$$

$$\overline{A}' = \frac{1}{|N'|} \sum_{i \in N} \bar{I}'[i]$$

$$\tilde{A} = (\overline{A} + \overline{A}')/2$$

$$P_1 = \frac{\overline{\sigma}}{\sigma}, P_2 = A, P_3 = \tilde{A} - \overline{A};$$

$$P_1' = \frac{\overline{\sigma}}{\sigma'}, P_2' = A', P_3' = \tilde{A} - \overline{A}'$$